

Non-Linear Interaction Mechanisms of an Ultra-Intense Laser Pulse with an Underdense Plasma

ADAM Jean C., HERON Anne, LAVAL Guy and MORA Patrick
Centre de Physique Théorique, CNRS-Ecole Polytechnique, Palaiseau, France

(Received: 26 January 1999 / Accepted: 11 August 1999)

Abstract

The interaction of an intense beam ($10^{19} < I < 10^{20} \text{W/cm}^2$) with moderately dense plasmas has been investigated by using theoretical analysis as well as numerical simulations. The parametric instabilities of a plane intense light wave have been theoretically studied in this strongly coupled case, with a particular emphasis on filamentation and the generalization of the TPD instability. Then these results are used to discuss numerical simulations. A 2D PIC code is used to study the propagation of picosecond pulses. The theoretical conclusions may be compared with present experimental results. These experiments show that the plasma strongly absorbs the intense radiation for densities where it would be expected to be transparent or reflective via Raman instabilities. Moreover, very high electron temperatures are achieved and multi-MeV particles are generated. These behaviors result from the strong non-linear interaction of the radiation with the plasma.

Keywords:

relativistic plasma, laser-plasma interaction, absorption, MeV electrons

1. Introduction

The chirped pulse amplification of laser light has opened a new field of investigation for plasma physicists. Laser peak powers have reached up to one petawatt. By focusing this light beam, intensities larger than 10^{20}W/cm^2 are now available. In this intensity range, the electrons are brought to relativistic energies by the mere oscillation in the laser electric field. Consequently, the physics of laser plasma interaction is strongly modified. The electron mass depends on the light intensity and the usual picture of wave propagation does not apply any more to this relativistic plasma.

A large number of ultra-high intensity lasers have been built to generate high energy particles for several purposes. Among them, the fast ignition of fusion targets raised great hopes by lowering the laser required energy to obtain the fuel burning and a thermonuclear gain. The fast ignition principle relies upon the

assumption that the oscillating electrons can be converted into a high energy particle beam which will heat the dense core of a compressed pellet. Preliminary experiments and numerical simulations show that the conversion does occur when the ultra-intense laser beam interacts with a very overdense plasma.

However, several physics issues have to be examined before being able to make a realistic assessment of the method. Among them, the channeling of the ultra-intense pulse through the underdense corona is challenging. The short intense pulse has to propagate through the long coronal plasma without deviation, filamentation and absorption. The current solution implies that a long intense prepulse will drill a channel in the coronal plasma. Once this channel formed, the ultra-intense pulse will reach safely the dense core.

In order to define the desirable parameters of the

Corresponding author's e-mail: adam@cph.t.polytechnique.fr

residual plasma inside the channel, it is necessary to know how the ultra-intense pulse will interact with it. This is the purpose of several experiments in which an ultra-intense pulse interacts with a preformed underdense or slightly overdense plasma. In these experiments, anomalous absorption has been observed [1] as well as a strong reduction of the transmission through moderately underdense plasmas. For the same parameters, high energy electrons have been detected.

In this paper, the interaction of an ultra-intense 1 μm laser pulse with moderately dense plasmas will be investigated by using mainly 2D numerical particle simulations. The transmission, reflection and absorption of the pulse will be studied for densities in the range $n/n_c = 0.05 - 0.4$ and for intensities from 10^{16} to 10^{20}W/cm^2 . The results will then be discussed in the light of theoretical calculations, mainly about the parametric instabilities in the strongly relativistic regime. It will be shown that the interaction is strongly non-linear and may be understood by assuming that the laser plasma interaction leads to a bulk electron heating to relativistic energies. Calculations of parametric instabilities in such hot plasma will be necessary in order to understand the numerical results.

2. Numerical Simulations

In the numerical simulations, the electromagnetic field is propagated by integrating the full Maxwell equations. The electromagnetic wave is linearly polarized with the electric field in the plane of incidence. In order to simulate a focused beam, the intensity profile is assumed to be gaussian with the same $5 \lambda_0$ full width at half maximum (FWHM) for all cases, where λ_0 is the vacuum wavelength. For the plasma, 2D particle-in-cell simulations are used [2-3]. The simulation box initially contains a plasma slab, with sharp edges normal to the direction of incidence of the laser. The slab width is $200 \lambda_0$ and in the transverse direction, normal to the direction of incidence, the simulation box is $73 \lambda_0$ wide. There are 74 million particles and 8.4 million grid points. The boundary conditions are periodic in the transverse direction. In order to avoid interaction between the simulation and its periodic images, the particles are cooled as they cross the transverse boundary. In front of the plasma slab, the length of the vacuum region is $35 \lambda_0$. The electron/ion mass ratio is $1/1836$ and the initial temperature is 1 KeV. The temporal pulse shape is approximately gaussian with a full width at half maximum $\Delta T = 1200 \omega_0^{-1}$ where $\omega_0 = \pi c/\lambda_0$. A series of simulations have

been performed with $0.05 < n/n_c < 0.4$ and $10^{16} < I_m < 10^{20} \text{W/cm}^2$ where I_m is the maximum intensity of the pulse. In this range of intensities, the relativistic mass factor γ of an electron oscillating in the laser field varies from 1.01 to 6.1 for a 1 μm radiation. The transmission and the reflection coefficients were obtained by computing the outgoing flux of the Poynting vector through the simulation box boundaries and the absorption coefficient was given by the overall energy flux balance. One run lasts 15 hours on the 64 processors of a T3E.

Figures 1-a,b,c are plots of the transmission,

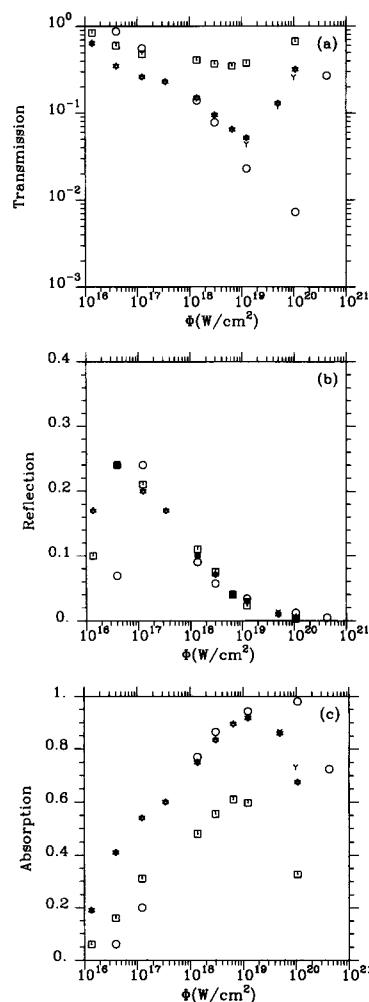


Fig. 1 a) Transmission coefficient as a function of flux for three different densities of plasma ($\square n/n_e = 0.1$, $*$ $n/n_e = 0.2$, $\circ n/n_e = 0.4$, $\gamma n/n_e = 0.4$ and fixed ions), b) Reflection coefficient as a function of flux for the same parameters as figure 1a), c) Absorption coefficient as a function of flux for the same parameters as figure 1a).

reflection and absorption coefficients as a function of I_m for three different density ratios n/n_c . These results show that the transmission initially decreases with I_m , becoming very low at $I_m = 10^{19} \text{W/cm}^2$ for $n/n_c = 0.2$ or $n/n_c = 0.4$ and increasing again for $I_m > 10^{19} \text{W/cm}^2$, to reach 30% for $I_m = 10^{20} \text{W/cm}^2$.

The rather large transmission at very high intensities could result from the action of the ponderomotive force which creates a hollow density channel where the laser propagates without interaction with the plasma. In order to check this interpretation, simulations have been performed with fixed ions for $I_m > 10^{19} \text{W/cm}^2$. It is seen, on figure 1-a, that there is no significant modification of the transmission in this case. Consequently, this simple interpretation does not seem to apply. Instead, it suggests that the low transmission results from an interaction taking place in the front of the pulse where the electrons have not yet been evacuated.

The reflection coefficient reaches 0.25 for fluxes in the 10^{17}W/cm^2 range and falls down for higher fluxes to negligible values for $I_m = 10^{20} \text{W/cm}^2$. The behavior of the reflection coefficient for $n/n_c = 0.4$ is enlightening: for $I_m < 10^{17} \text{W/cm}^2$, the reflection coefficient is much smaller than for lower densities, as it is expected since backward Raman instabilities are forbidden. At higher intensities, relativistic effects allow again Raman instabilities [4] and the reflection coefficient behaves in the same way as for lower densities.

The absorption coefficient brings out the surprisingly strong energy transfer between the electromagnetic wave and the plasma in the relativistic regime $I_m > 10^{18} \text{W/cm}^2$, whereas, at lower fluxes and in this density range, the absorption is very low, as predicted from the linear propagation theory. The anomalous absorption is not modified if the ions are fixed, at least for $I_m > 10^{18} \text{W/cm}^2$. It rules out the radial acceleration of ions by the ponderomotive potential as the origin of the anomalous absorption. The main purpose of this work is to try to understand this relativistic induced opacity.

Figures 2-a,b,c are plots of the transmission, reflection and absorption coefficients as a function of n/n_c for three different values of I_m in the relativistic regime. The very fast growth of the absorption coefficient with density excludes a direct acceleration of electrons by the laser since it would lead to a linear growth of the absorption coefficient with the density. It implies that the heating process is very sensitive to the plasma density. It also shows that experimental results

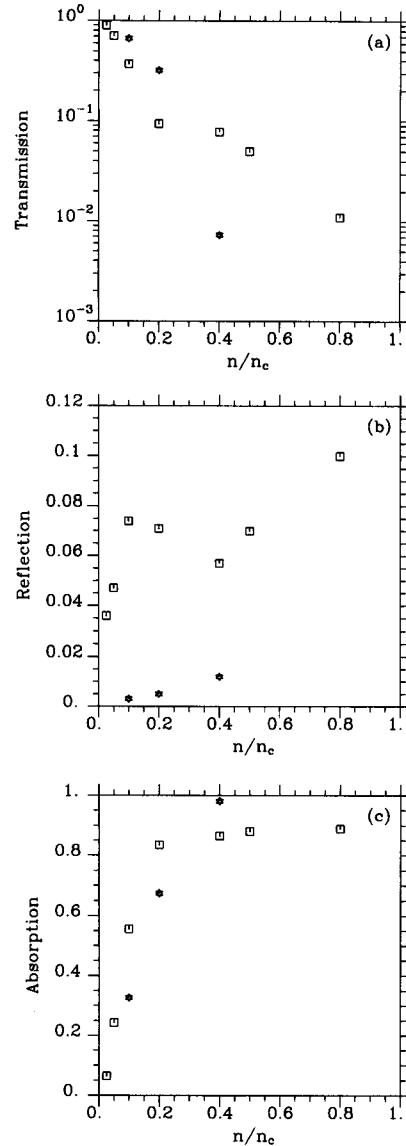


Fig. 2 a) Transmission coefficient as a function of density of plasma for two different fluxes (\square 3.10^{18}W/cm^2 , $*$ 10^{20}W/cm^2), b) Reflection coefficient as a function of density of plasma for the same parameters as figure 2a), c) Absorption coefficient as a function of density of plasma for the same parameters as figure 2a).

can be widely scattered if the plasma density is not controlled with a sufficient precision.

The importance of transverse effects is clear on figure 3 where the distribution of the laser intensity has been plotted at a given time. As already noticed [5], it is seen that strong self-focusing may occur and filamentation takes place even for such narrow beams.

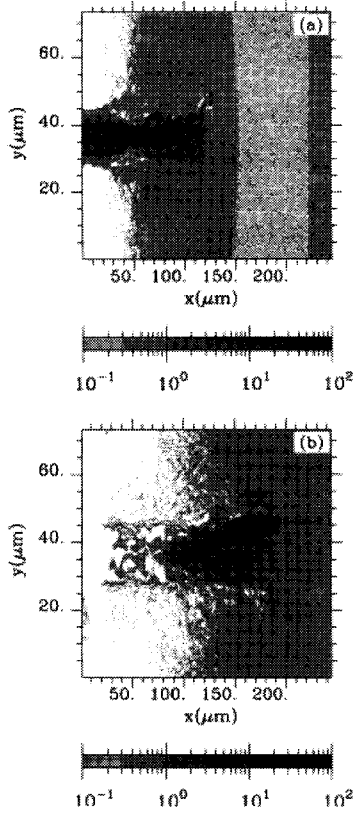


Fig. 3 Isovalues of the flux of the Poynting vector across the y direction in dimensionless units for $n/n_e = 0.2$ and 10^{20} W/cm 2 at two different times a) 500fs, b) 840fs.

These transverse processes have to be taken into account in any explanation of the strong absorption since 1D simulations exhibit a much higher transparency [6].

3. Parametric Instabilities

In the relativistic regime, parametric instabilities cannot be studied by using the resonant weak coupling approximation. The laser wave propagation is non-linear and simple solutions are available only for circular polarization. In such a case and for a cold plasma, the stability of the solution with respect to longitudinal perturbation has been thoroughly investigated [4]. In the relativistic regime and for $0.05 < n/n_e < 0.4$, the usual forward and backward branches of the Raman stimulated scattering merge into a mixed instability in which the Stokes and the anti-Stokes waves are strongly coupled. The growth rate peaks for modes such that the Stokes component is backscattered. Moreover the growth rate is very high as indicated on figure 4. In this figure, the maximum growth rate is plotted as a function of the intensity as well as the corresponding plasma wave number k , its frequency ω and its phase velocity v_ϕ . The growth rates and frequency unit is the laser pulsation ω_0 , the wavenumber unit is the laser light wavenumber in vacuum k_0 and the phase velocity unit is the velocity of light c . In these units, the frequency of the Stokes component is $1-\omega$ and its wavenumber is $1-k$. For intensities larger than 10^{19} W/cm 2 , it is seen that $k =$

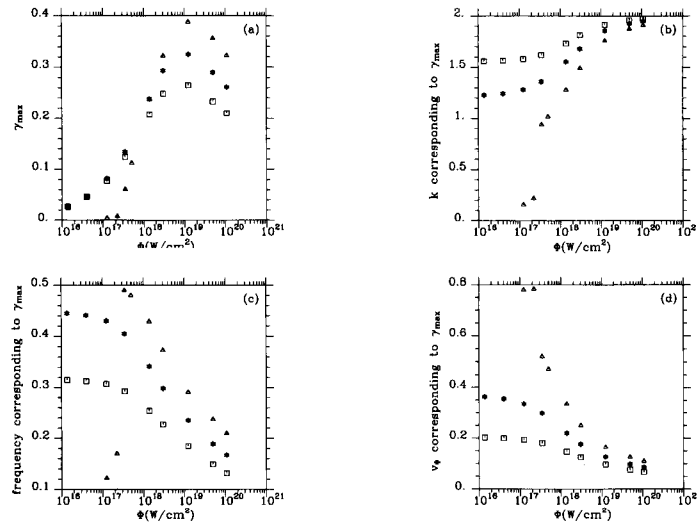


Fig. 4 Solutions of the cold dispersion relation as a function of flux for three different densities of plasma (\square $n/n_e = 0.1$, $*$ $n/n_e = 0.2$, Δ $n/n_e = 0.4$), a) the maximum of the growth rate, b) the wave number corresponding to the maximum growth rate, c) the real part of the frequency corresponding to the maximum growth rate, d) the phase velocity corresponding to the maximum growth rate.

2 while ω and v_ϕ become very small. These features are those of the backward Raman instability in a very low density plasma. It can be understood by noticing that the relativistic increase of the electron mass brings down the effective plasma frequency. However and on the contrary, the growth rate is very high since it peaks at 0.4 for $n/n_c = 0.4$ and reaches 0.26 for $n/n_c = 0.1$. This values are larger than the effective plasma frequency ω_p/γ . It implies that the Raman instability is in the direct Compton regime. It is also seen that the absorption coefficient follows nicely the growth rate dependence on the intensity. Consequently, it is natural to link the observed large absorption to the parametric instability in the relativistic regime.

4. Electron Heating

If the reflectivity is now considered, the picture does not fit so well the results, since the instability is essentially a stimulated backward scattering which should generate a strong reflection. In order to explain this discrepancy, the very fast growth of the instability and the very low phase velocity of the plasma wave have to be taken into account. These features show that, after a few femtoseconds, wavebreaking will occur for

the longitudinal perturbation, leading to an efficient longitudinal heating of the electrons. This heating should stabilize the backward modes with low phase velocity. Such stabilization of the backward Raman scattering has already been observed in experiments [7], where the bursting of the reflected light was interpreted as signs of the wavebreaking for the longitudinal perturbation.

In order to settle this point in a more quantitative way, the parametric instability dispersion equation has been established for longitudinally heated plasmas [4] and solved numerically. The unperturbed electron distribution function in momentum space is assumed to be cold in the transverse direction. As regards the longitudinal velocity dependence, the distribution function is the sum of a dirac function and of a gaussian with a zero average momentum and a rms momentum δ in mc units, which is supposed to take into account the formation of hot tail. It has been found that a hot tail does not modify the instability, even when it contains 20% of the particles. Consequently, only distributions with 100% hot particles will be considered here.

Figure 5 shows that for an intensity $I = 3 \times 10^{18} \text{ W/cm}^2$ and $n/n_c = 0.2$, the maximum growth rate is only

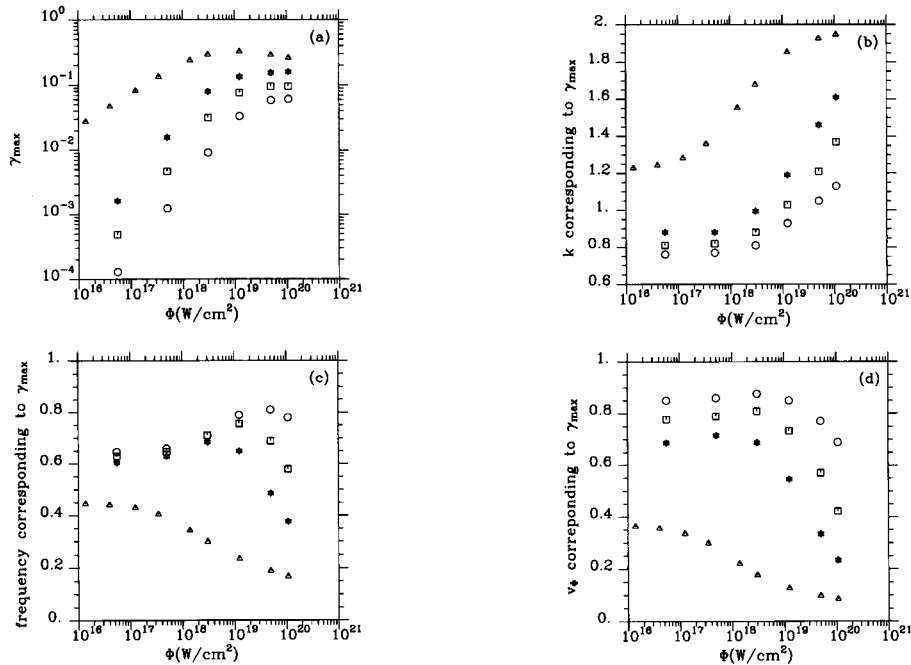


Fig. 5 Solution of the warm dispersion relation as a function of flux for $n/n_c = 0.2$ and different values of the «thermal» spread ($\Delta \delta = 0.$, $\ast \delta = 1.$, $\square \delta = 2.$, $\circ \delta = 4.$), a) the maximum of the growth rate, b) the wave number corresponding to the maximum growth rate, c) the real part of the frequency corresponding to the maximum growth rate, d) the phase velocity corresponding to the maximum growth rate.

0.06 for $\delta = 1$ and there is no more backscattering. For larger δ , the growth rate decreases and it becomes negligible for $\delta > 3$. It is noticed that, for $\delta = 1$ the phase velocity is 0.8 in c units, which implies that the longitudinal wave is strongly damped. In this case and for hotter plasmas, the laser pulse is scattered and absorbed by a strong kinetic stimulated Compton scattering with a large frequency shift. At high intensity, the backscattering is ruled out and the growth rate becomes negligible for much higher values of δ . This is confirmed by the PIC simulations which show that the average electron energy, in the pulse, is 3 MeV for $I = 3 \times 10^{18} \text{ W/cm}^2$, while it peaks at 20 MeV for $I = 10^{20} \text{ W/cm}^2$.

5. Transverse Effects

Transverse effects have been studied theoretically in the cold plasma case [8]. It has been shown that the instability features of the 1D case extends in the transverse direction, so that instabilities with large transverse mode numbers are expected to be excited at the same level as the purely longitudinal modes. However, the growth rate peaks always for purely longitudinal wavenumbers. In the simulations, these oblique modes are found to have amplitudes lower than the parallel ones but they are responsible for the observed transverse heating which is slightly smaller than in the longitudinal direction. The absorption is much larger in 2D simulations than in 1D simulations. This increase cannot be explained only by the transverse heating. The oblique modes could have also an efficient effect on the longitudinal heating by destroying the distribution function plateau which would be formed in a short time with purely 1D longitudinal modes, avoiding then a saturation of the heating mechanism and

allowing to reach very high average energies.

6. Conclusions

Numerical simulations have shown that moderately dense plasmas absorb efficiently short pulses of laser light in the relativistic regime. This anomalous absorption seems to be linked to the excitation of strong Raman-type parametric instabilities. These instabilities lead to a bulk heating of the electrons which stabilizes the backward scattering instability and leaves stimulated Compton scattering instabilities to further heat the electrons to relativistic energies.

The intensity, the pulse duration and the plasma density have been chosen in ranges corresponding to present experiments and fitting the current capacity of the numerical simulations. It is not yet possible to draw conclusions for the conditions of fast ignition. However, it indicates already that the main pulse may loose energy if the preformed channel still contains a low density plasma.

References

- [1] J.A. Cobble *et al.*, *Phys. Plasmas* **4**, 3006 (1996).
- [2] A.B. Langdon, B. Lasinski, in *Methods of Computational Physics* (Academic Press, New York, 1976) Vol. 9, p. 327.
- [3] J.C. Adam *et al.*, *J. of Comput. Phys.* **47**, 2 (1982).
- [4] S. Guerin *et al.*, *Phys. Plasmas* **2**, 2807 (1995).
- [5] A. Pukhov and J. Meyer-ter-Vehn, *Phys. Rev. Lett.* **76**, 3975 (1996).
- [6] J.C. Adam *et al.*, *Phys. Rev. Lett.* **78**, 4765 (1997).
- [7] C.A. Coverdale *et al.*, *Phys. Rev. Lett.* **74**, 4659 (1995); A. Modena *et al.*, *Nature*, **377**, 606 (1995).
- [8] B. Quesnel *et al.*, *Phys. Rev. Lett.* **78**, 2132 (1997).